Contribution of an Active Site Cation−π Interaction to the Spectroscopic Properties and Catalytic Function of Protein Tyrosine Kinase Csk†

Sungsoo Lee,‡ Xiaofeng Lin,‡ John McMurray,§ and Gongqin Sun*,‡

Department of Cell and Molecular Biology, University of Rhode Island, Kingston, Rhode Island 02881, and Department of Neuro-Oncology, M. D. Anderson Cancer Center, Houston, Texas 77030

Received July 11, 2002; Revised Manuscript Received August 8, 2002

ABSTRACT: Csk is a soluble protein tyrosine kinase that phosphorylates and negatively regulates protein tyrosine kinases of the Src family. The spectral properties of the intrinsic Trp fluorescence of Csk and their underlying structural features were investigated in combination with urea denaturation and site-specific mutagenesis. It was found that W352 contributed approximately 35% of the total Trp fluorescence of Csk even though seven other Trp residues were present. The enhanced contribution by W352 to Csk fluorescence was due to an interaction between its indole ring and the positively charged guanidino group of R318. W352 is located on the peptide substrate binding P+1 loop, and R318 is located on the catalytic loop. The W352−R318 interaction, called a cation−π interaction, uniquely couples the two loops in the active site. Mutations that disrupted this coupling resulted in varying levels of decreases in Csk activity, and consistent and significant increases in K_m values for its physiological substrate, Src protein tyrosine kinase. These results indicated that structural coupling between the two loops by the cation−π interaction played an important role in Csk substrate binding. Since both R318 and W352 are highly conserved among protein tyrosine kinases, this cation−π interaction is likely a signature structural feature of most, if not all, PTKs. These studies elucidated the roles of two conserved signature residues in Csk and formed a baseline for further structure−function studies of Csk and other PTKs.

Protein tyrosine kinases (PTKs)[1] are a large family of enzymes that catalyze the phosphorylation of specific Tyr residues in selected protein substrates (*1*). This posttranslational modification alters the properties of the substrate proteins and is a key mechanism in cellular signal transduction. Due to their critical roles in cell signaling and the correlation between their activity and disease processes of the cell, many PTKs are targets for inhibitor development (*2*). For the purposes of understanding their mechanisms in signal transduction and developing PTK inhibitors for therapeutic applications, establishing the structure−function relationships of PTKs is an important area of research.

Csk is a soluble PTK that phosphorylates and negatively regulates the function of PTKs in the Src family (*3*, *4*). Due to its ease of expression, its lack of autophosphorylation, and its relatively simple structure, Csk has emerged as a model in understanding PTK structure−function relationships (*5*, *6*). Csk contains an SH3, an SH2, and a catalytic domain in the order of N- to C-terminus (Figure 1A) (*7*). The catalytic domain of Csk (Figure 1B) is similar to those of all other PTKs in overall structure, and consists of two lobes: the N-terminal lobe that binds ATP−Mg substrate, and the C-terminal lobe that binds the protein substrate (*8*). The cleft between the two lobes is the active site, where phosphoryl transfer occurs during catalysis. The active site cleft contains two loop structures: the catalytic loop and the activation loop. The catalytic loop of Csk, like those of most PTKs, contains the following sequence: His^{312}-Arg-Asp-Leu-Ala-Ala-Arg-Asn^{319}. Most of the catalytic loop residues are highly conserved and are believed to be critical for catalysis. The activation loop is usually 15−21 residues long, starts with a highly conserved Asp^{332}-Phe-Gly motif on the N-terminal end, and is followed by the P+1 loop located on the peptide binding lobe. The activation loop often contains one or multiple Tyr residues as the autophosphorylation site-(s) (*9*). Autophosphorylation of such residue(s) leads to activation of the kinases (*10*). PTKs of the Csk family (Csk and Chk) are exceptions in that their equivalent loops do not contain a Tyr residue (*7*, *11*). The Csk P+1 loop has the sequence of Lys^{347}-Leu-Pro-Val-Lys-Trp-Thr-Ala-Pro-Glu^{356}. Many residues in this loop are also highly conserved among PTKs. Several residues in the P+1 loop in other PTKs, and likely in Csk as well, form the surface for peptide substrate binding (*12*).

Although crystal structures of a number of PTKs have been solved (*8*, *12*−*18*), detailed structure−function relationships in the active site have not been established. PTKs often exist in multiple regulated forms, further complicating our understanding of their structure−function relationships (*19*). In addition to autophosphorylation, other mechanisms such

† This work was supported by grants from the NIH (1 P20 RR16457) and the University of Rhode Island Research Council.

* Correspondence should be addressed to this author at the Department of Cell and Molecular Biology, 117 Morrill Science Building, 45 Lower College Rd., University of Rhode Island, Kingston, RI 02881. Phone: (401) 874-5937, FAX: (401) 874-2202, E-mail: gsun@uri.edu.

‡ University of Rhode Island.

§ M. D. Anderson Cancer Center.

[1] Abbreviations: F_t, total integrated fluorescence; GST, glutathione *S*-transferase; IRK, insulin receptor kinase; kdSrc, kinase-defective Src that contains a K295M mutation; λ_{max}, wavelength of maximal fluorescence emission; PTK, protein tyrosine kinase.

10.1021/bi026439g CCC: $22.00
Published on Web 09/13/2002

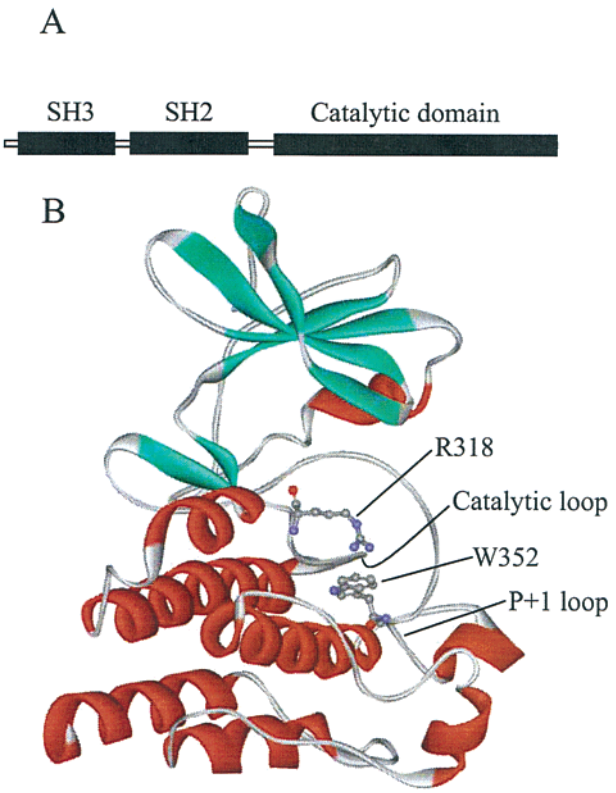

FIGURE 1: Structure of Csk. (A) A diagram illustrating Csk structural organization. (B) Tertiary structure of the catalytic domain of Csk. The coordinates for the structure were obtained from the Protein DataBank (1BYG), and the picture was generated using WebLab Viewer (Molecular Simulations Inc.). The catalytic and P+1 loops are indicated. R318 and W352 residues are represented in ball-and-stick and are labeled.

as trans-phosphorylation on other specific Tyr, Ser, and Thr residues, and association of the regulatory domains to their respective ligands also regulate the structure and function of the kinase domains (*20*). Elucidation of the relationships between the dynamic conformational changes and the kinase function is an important aspect of structure−function studies.

The fluorescence of Trp is extremely sensitive to its environment. Intrinsic Trp fluorescence can often be used as a sensitive reporter for the conformational changes of an enzyme as a result of its binding to substrates, inhibitors, or other ligands, or due to covalent regulatory modifications. This technique in combination with site-specific mutagenesis and chemical denaturation has been used to elucidate structure−function relationships of a large number of proteins and enzymes (*21*−*24*), but rarely applied to studying PTKs (*25*). However, these techniques may be particularly useful in characterizing the dynamic conformational changes associated with catalysis and regulation of PTKs. In this report, we applied these techniques to investigate the spectral and structural properties of Csk. These studies form a baseline for further investigation of the catalytic and regulatory dynamics in Csk and other PTKs.

EXPERIMENTAL PROCEDURES

Chemicals and Reagents. All reagents used for bacterial culture and protein expression were purchased from Fisher. Chromatographic resins, glutathione-agarose, iminodiacetic acid-agarose, and Sephadex G25 were purchased from Sigma. DNA primers were synthesized by Integrated DNA Technologies. [γ-^{32}P]ATP (6000 Ci mol^{-1}) was purchased from PerkinElmer.

Recombinant Kinase Expression and Site-Specific Mutagenesis. Wild-type Csk was expressed in *E. coli* (DH5α) using pGEX-Csk-st plasmid (*26*, *27*). Site-specific mutants were generated using QuikChange (Stratagene). The entire coding regions of the mutant plasmids were sequenced to confirm that the correct mutations were incorporated. The glutathione *S*-transferase (GST)−Csk fusion proteins were purified by glutathione affinity chromatography (*27*, *28*). GST and Csk were separated by thrombin digestion on the affinity column (*28*) in 50 mM Tris-HCl, pH 8.0. The Csk released from GST by thrombin digestion was eluted with 50 mM Tris-HCl, pH 8.0, and stored at −80 °C in aliquots.

The chicken Src mutant devoid of kinase activity (kdSrc, Src-K295M) was coexpressed with GroEL and GroES chaperone in BL21(DE3) as previously described (*29*). It has been previously shown that K295M mutation abolished the Src kinase activity, but did not affect its ability to serve as a substrate for Csk (*29*, *30*).

Kinase Activity Assays. The kinase activity of Csk and mutants was determined using kdSrc and [γ-^{32}P]ATP (600 dpm pmol^{-1}) as the substrates as described previously (*31*). Briefly, phosphorylation reactions were performed in 50 μL volumes at 30 °C in the protein kinase assay buffer: 50 mM Tris-HCl (pH 8.0) containing 5% glycerol, 0.005% Triton X-100, 0.05% 2-mercaptoethanol. The standard assay used 2 mM $MnCl_2$, 0.2 mM ATP, and 8 μM kdSrc. After a 10 min reaction time, 35 μL of the reaction mixture was spotted onto Whatman filter paper squares (1 × 1 cm), which were washed in 5% TCA at 65 °C 3 times at 10 min each. The radioactivity incorporated into kdSrc was determined by liquid scintillation counting. For each assay reaction, a background control, in which all reaction components except kdSrc were present, was used to correct for nonspecific phosphorylation, Csk autophosphorylation, and washing background. Assays were performed in duplicate, and each assay was repeated at least twice with reproducible results.

To determine the catalytic parameters of Csk using kdSrc as a substrate, 1−10 μM kdSrc was used as the variable substrate. The K_m and V_{max} values were determined using a double-reciprocal plot as described earlier (*31*).

Urea Denaturation and Intrinsic Trp Fluorescence. All fluorescence determinations were performed on a Perkin-Elmer LS55 luminescence spectrometer at 25 °C. To minimize the contribution of Tyr and Phe residues to the fluorescence, an excitation wavelength of 295 nm was used (*25*). Csk at 0.5 μM was mixed with the given concentrations of urea in 50 mM Tris-HCl, pH 8.0, and incubated at 25 °C for 1 h. The emission spectra from 320 to 420 nm were recorded. Integrated fluorescence was calculated using the FL WinLab software (PerkinElmer) and reported as a measure of the total fluorescence intensity (F_t). The wavelength of maximum emission for each spectrum (λ_{max}) was manually determined from the spectrum.

RESULTS

Initial Characterizations of the Intrinsic Trp Fluorescence of Csk. Csk contains eight Trp residues, two (W8 and W47) in the SH3 domain, one (W82) in the SH2 domain, and five

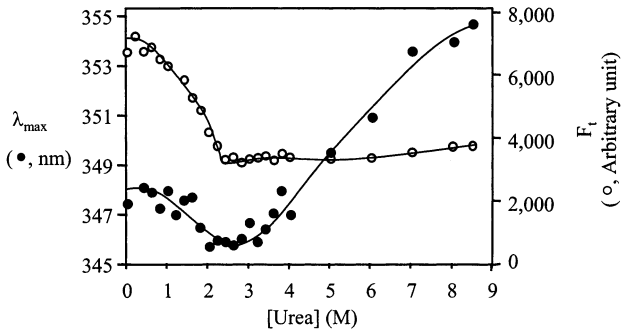

FIGURE 2: Denaturation profile of Csk. Csk (0.5 μM) was incubated in 50 mM Tris-HCl, pH 8.0, and different concentrations of urea ranging from 0 to 8.5 M at 25 °C for 1 h. The spectra of Csk samples at the end of incubation were recorded. The λ_{max} (closed circles) of each spectrum was determined manually from the spectrum, and F_t (open circles) was calculated using the FL WinLab software.

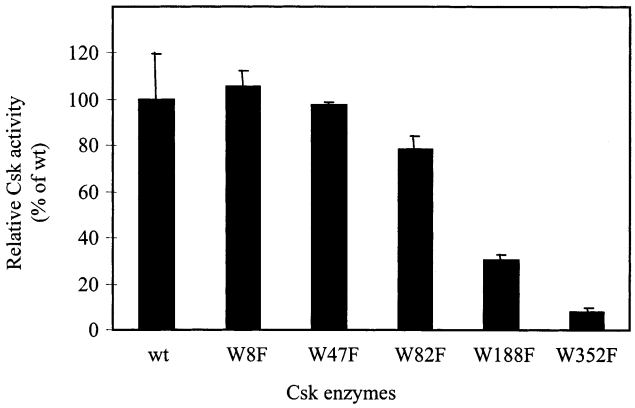

FIGURE 3: Relative kinase activities of Trp to Phe mutants of Csk. Kinase activities of Trp to Phe mutants of Csk were determined using kdSrc as the protein substrate (8 μM). The activity of wt Csk was taken as 100%. Standard errors are shown as error bars.

(W188, W352, W370, W377, and W423) in the catalytic domain. As the first step of establishing spectral properties of Csk, we determined its intrinsic Trp fluorescence spectrum and how urea unfolding affected the spectrum. Native Csk had a fluorescence emission spectrum typical for a protein with a λ_{max} of 348 nm (data not shown). The λ_{max} of 348 nm was significantly shorter than λ_{max} values of 355−360 nm for free Trp amino acid, indicating that these Trp residues in Csk were located in relatively hydrophobic environments. In comparison, the Csk sample incubated with 8.5 M urea had a markedly different spectrum. The denatured Csk had an F_t about 50% of that of native Csk, and an emission maximum of 355 nm, red-shifted by 7 nm compared to that of the native Csk. The red shift in λ_{max} indicated that urea treatment exposed the Trp residues to more polar environments. The λ_{max} of 355 nm for the urea-treated Csk was identical to that of a Trp-containing peptide in aqueous solution (*23*), suggesting that incubation with 8.5 M urea resulted in complete unfolding of Csk.

Gradual unfolding by increasing urea concentration can resolve a protein structure into different substructures according to their sensitivity to urea denaturation (*32*). The changes of F_t and λ_{max} of Csk as functions of urea concentration can be divided into two distinct phases (Figure 2). The first phase occurred in the range of 0−2.5 M urea, and was characterized by a 50% decrease in F_t and a 2 nm blue shift in λ_{max}. Both the large decrease in F_t and the blue shift in λ_{max} indicated that certain Trp residue(s) underwent profound changes in its (their) environment as a result of incubation with up to 2.5 M urea. The large decrease in F_t was consistent with two possibilities: either Trp fluorescence was enhanced in native Csk or it was quenched in 2.5 M urea-treated Csk. The first possibility was considered more plausible, since it was more likely that one or a few Trp residues were located in a fluorescence-enhancing environment in native Csk. On the other hand, it is difficult to envision a conformational change that could result in 50% quenching of the total fluorescence of eight Trp residues located in different domains without unfolding the protein. The blue shift indicated that the environment of some Trp residues became more hydrophobic upon incubation with up to 2.5 M urea. The lack of red shift in λ_{max} in this phase indicated that hydrophobic core structures that harbored the Trp residues were not unfolded.

The second phase occurred in the range of 2.5−8.5 M urea. This phase exhibited a slow and gradual increase in F_t and a simultaneous red shift in λ_{max} from 346 to 355 nm. The red shift in λ_{max} suggested a gradual increase in exposure of Trp residues to the aqueous environment, indicative of an unfolding of the hydrophobic core of Csk structure. Based on this biphasic denaturation, the conformational changes in the first phase likely represented disruption of interactions that were unique to either Csk itself or the kinase structure in general. We decided to further investigate the structural bases for these conformational changes.

Trp352 Had an Enhanced and Red-Shifted Emission Spectrum. To identify the Trp residue(s) whose fluorescence was sensitive to the conformational changes in the first phase, each of the eight Trp residues in Csk was individually mutated to Phe. The expression levels and purified yields for five (W8F, W47F, W82F, W188F, and W352F) of the mutants were comparable to those for wt Csk. The other three mutants (W370F, W377F, and W423F) were expressed in *E. coli*, but did not bind to GSH-agarose columns. The lack of binding by these mutants was likely due to incorrect folding or lack of stability. These three Trp residues are located in the hydrophobic core of the peptide binding lobe (*8*, *33*), and may play essential roles for the correct folding of the kinase.

Mutations of W8, W47, and W82 had relatively minor effects on the specific activity of Csk, suggesting that these mutations did not result in global misfolding of the Csk protein (Figure 3). W188F and W352F mutations decreased the activity by 70% and 90%, respectively. The retention of at least 10% of the wt activity argued against the possibility that any of these mutations caused gross misfolding of the mutants. In the absence of global structural disturbance, it is unlikely that the mutations affected the fluorescence contributions of other Trp residues. This consideration allows us to assess the apparent contribution of fluorescence by each of the mutated residues.

Mutation of W8, W47, W82, or W188 to Phe did not change the λ_{max}, and decreased F_t to various extents, by as low as 4% for W82F and as much as 13% for W8F (Figure 4A). Mutation of W352F had a much more striking effect on both the emission intensity and the λ_{max}, decreasing the former by 35% and shifting the latter by 6 nm from 348 nm for wt to 342 nm for the mutant. The apparent fluorescence

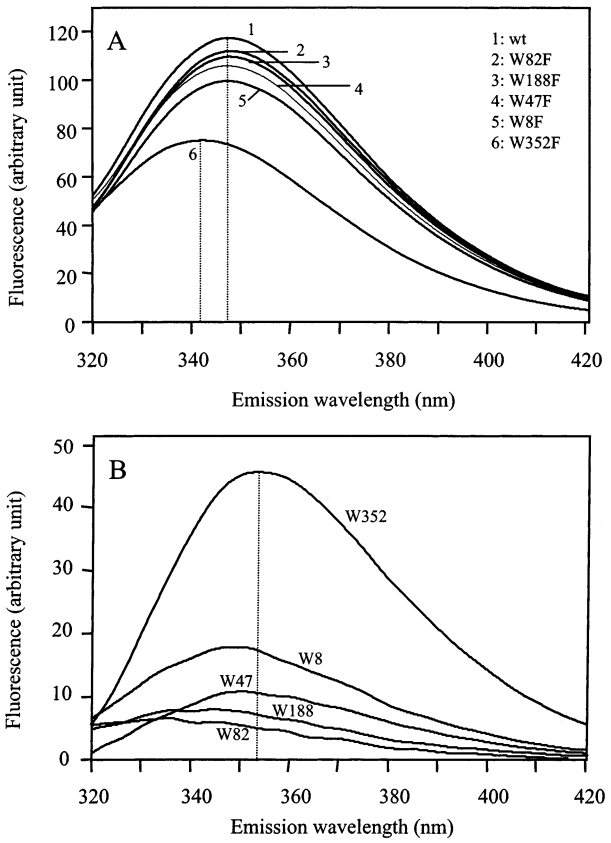

FIGURE 4: Fluorescence spectra of wt and Trp to Phe mutants of Csk and calculated spectra of individual Trp residues. (A) Fluorescence spectra of wt and Csk mutants. The dashed lines were added to highlight the difference in λ_{max} of W352F with other Trp to Phe mutants and the wt. (B) Fluorescence spectra of individual Trp residues determined by subtracting the spectra of individual Trp to Phe mutants from that of wt Csk. The λ_{max} of W352 emission, indicated by the dashed line, was significantly red-shifted compared to the spectra of other Trp residues.

spectrum of each Trp residue was determined by subtracting the fluorescence spectrum of each Trp mutant from that of wt Csk (*24*) (Figure 4B). It was evident that the apparent fluorescence spectrum of W352 was significantly higher in intensity, and significantly red-shifted in λ_{max}, compared to the "average" Trp residue in Csk. These spectral characteristics suggested that W352 was located in a highly rigid and hydrophilic environment.

To determine if W352 was the main fluorescent reporter of the conformational changes occurring in the first phase of Csk denaturation, we determined the denaturation profiles of W352F and other Trp to Phe mutants. The denaturation profiles of W8F (Figure 5) and other Trp to Phe mutants (data not shown) were virtually indistinguishable in both phases from that of wt Csk. In contrast, the denaturation profile of W352F is dramatically different. Both the large decrease in F_t and the blue shift in λ_{max} were absent in the denaturation profile of W352F, clearly indicating that W352 was the reporter of the conformational changes occurring in the first phase.

The Fluorescence Spectrum of W352 Is Enhanced and Red-Shifted by a Cation−π Interaction with R318. W352 is located in a conserved region of Csk called the P+1 loop. In the crystal structure of Csk, the indole ring of W352 apparently forms a cation−π interaction (*34*) with the

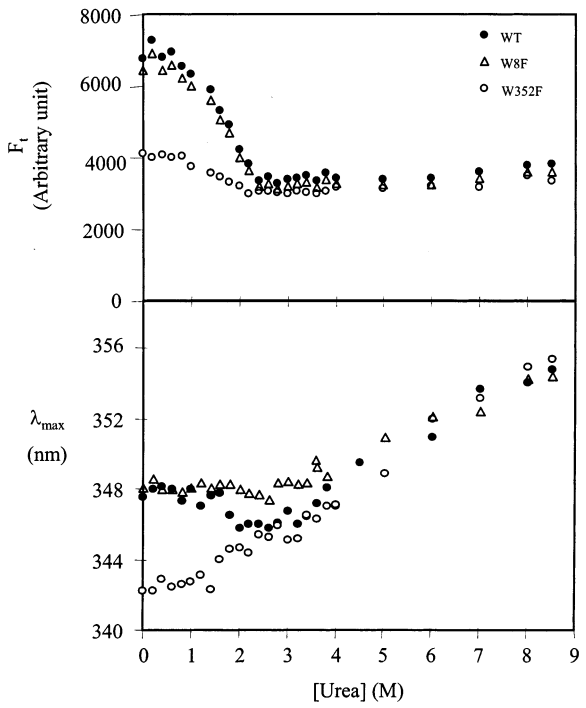

FIGURE 5: Denaturation profile of wt Csk, W8F, and W352F. The denaturation profiles were obtained as in Figure 2.

positively charged guanidino group of R318 from the catalytic loop (Figure 1B). This interaction likely provides a polar and rigid environment for W352, and would be consistent with the assignment of W352 as the main reporter of the conformational changes in the first phase of urea denaturation. The rigidity of the environment is likely responsible for the enhanced fluorescence intensity while the polarity of the environment is responsible for the longer λ_{max}. These analyses also implied that the conformational changes in the first phase of urea denaturation involved disruption of this cation−π interaction.

To test this hypothesis, we mutated R318 to Ala, which would be expected to remove the enhancement and red shift from the fluorescence of W352. The spectrum of R318A was compared to those of wt and W352F in Figure 6A. As expected, the fluorescence intensity of R318A was approximately 35% lower than that of the wt Csk, and closer to that of W352F. Furthermore the λ_{max} was blue-shifted by 3 nm (compared to wt Csk) to 345 nm, indicating that the side chain of R318 was responsible for the intensity enhancement and red shift in Csk Trp fluorescence. This result was consistent with our hypothesis that R318 enhanced and red-shifted the fluorescence of W352.

To test if the mutation of R318A only specifically affected the fluorescence of W352, but not that of other Trp residues, we generated a double mutant of R318A−W352F (Figure 6A). The emission spectrum of R318A−W352F was virtually identical to that of W352F, indicating that in the absence of W352, mutation of R318 to Ala had no detectable effect on the Csk fluorescence spectrum. This result demonstrated that R318 affected the fluorescence of only W352, but not other Trp residues. On the other hand, the similarity of the spectra of R318A−W352F and R318A indicated that in the absence of the positively charged side chain of R318, mutation of W352F caused only a minor decrease in F_t and a minor blue shift in λ_{max}. This result further demonstrated that the spectral

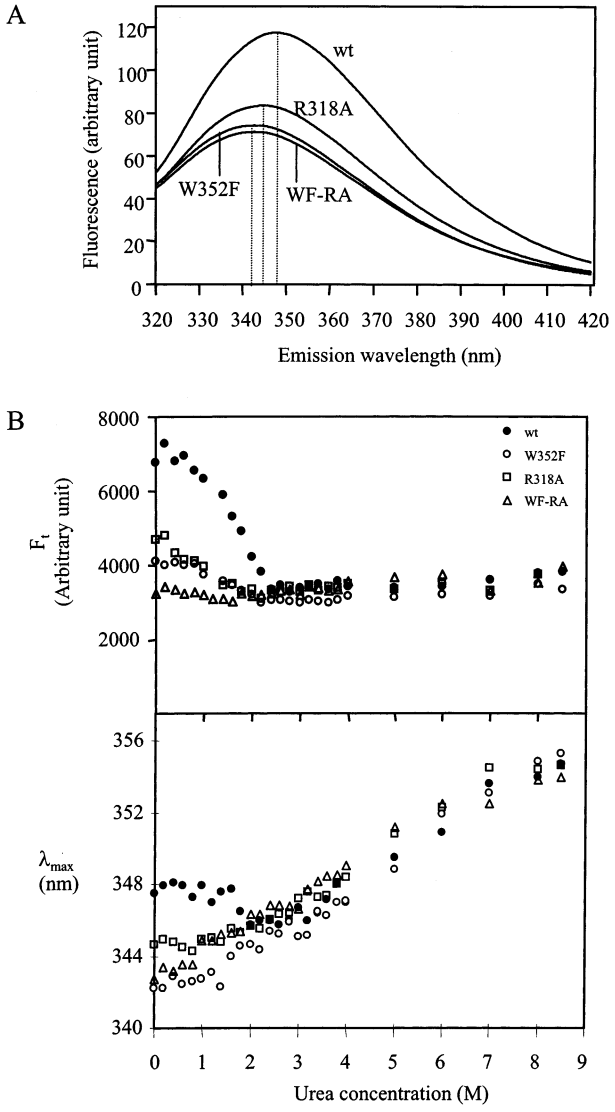

FIGURE 6: Cation−π interaction between W352 and R318 and spectral properties of Csk mutants in which the cation−π interaction was disrupted. (A) Spectra of wt and Csk mutants designed to disrupt the cation−π interaction between R318 and W352. Dashed lines were added to indicate the differences in λ_{max} among the mutants and wt Csk. WF−RA stands for the double mutant W352F−R318A. (B) Denaturation profiles of wt and cation−π interaction mutants of Csk.

properties of W352 were caused by the cation−π interaction with R318, not other interactions.

We next compared the denaturation profile of W352F, R318A, and R318A−W352F to wt Csk (Figure 6B). In the first phase, F_t of the mutants decreased slightly, but much smaller than the decrease in F_t for wt Csk. Furthermore, denaturation in the first phase did not result in a blue shift in λ_{max} for any of the three mutants. These data demonstrated that disruption of the cation−π interaction was largely responsible for the observed decrease in F_t and the blue shift in λ_{max} in the first phase of denaturation of wt Csk. The second phase of the denaturation profile was indistinguishable between the mutants and wt Csk, indicating that the unfolding of the hydrophobic core of Csk was not affected by the mutations that disrupted the cation−π interaction. From these results, we concluded that the cation−π interaction between W352 and R318 was responsible for the enhanced and red-shifted fluorescence of W352, which then acted as a reporter for the conformational changes in the first phase of denaturation.

Table 1: Catalytic Properties of Csk Mutants Disrupting the W352−R318 Cation−π Interaction

enzyme	k_{cat} (min^{-1})	$K_{m\ (kd-Src)}$ (μM)	$K_{m\ (ATP)}$ (μM)
wt	84.5 ± 8.8[a]	2.5 ± 0.05	97 ± 2
W352F	10.8 ± 0.3	46.1 ± 3.1	135 ± 20
R318A	0.5 ± 0.2	15.0 ± 4.0	357 ± 140
W352F−R318A	nd[b]	nd	nd
A316R−R318A	33.5 ± 1.3	23.8 ± 1.1	270 ± 2
W352A	19.9 ± 2.2	27.5 ± 3.0	188 ± 51
W352L	11.0 ± 0.6	17.5 ± 1.1	214.6 ± 46
W352E	ns[c]	ns	ns

[a] The numbers in parentheses are standard errors calculated from at least four assays. [b] nd: not detectable. Activity less than 0.1% of that of wt could not be reliably detected. [c] ns: the enzyme is not expressed in the soluble form in our expression system.

Function of the W352−R318 Cation−π Interaction. W352 is located on the highly conserved P+1 loop, and R318 is located on the catalytic loop. Considering the key functions for these loops, the demonstrated cation−π interaction between R318 and W352 would be expected to be critical for the catalytic function of Csk.

We addressed this issue by determining the catalytic parameters of Csk mutants that disrupted this cation−π interaction (Table 1). Csk specifically phosphorylates PTKs of the Src family on a C-terminal Tyr residue (Tyr527 in Src) and inactivates their kinase activity. To eliminate the intrinsic kinase activity of Src and use such a kinase-defective Src (kdSrc) as a substrate for Csk, we used a Src mutant in which Lys295 in the ATP binding domain was mutated to Met. It has been shown that this mutant had no kinase activity and served as good substrate for Csk (*29*).

The mutant W352F retained approximately 13 % wt activity (k_{cat}), without significantly affecting the K_m for ATP−Mg. On the other hand, the K_m for kdSrc increased 17-fold from 2.5 to 46.1 μM. The mutant of R318A retained only 0.6% of wt activity with a slightly increased K_m for ATP−Mg. The K_m for kdSrc was 5 times higher than that of wt. The effect on K_m by both R318A and W352F mutations suggested that the cation−π interaction between the catalytic loop and the P+1 loop was important for protein substrate binding.

Since mutation of W352 to Phe had much less effect on the kinase activity than R318A mutation (13% vs 0.6%), it was possible that F352 could partially fulfill the function of W352 by forming a cation−π interaction with R318. To test this possibility, we mutated W352 to Ala and Leu, two hydrophobic residues that could not form cation−π interaction with R318. Purified W352A and W352L had virtually identical catalytic parameters as W352F (Table 1), indicating that Phe did not form a functional cation−π interaction with R318. To determine if a salt bridge could replace the cation−π interaction, we also mutated W352 to Glu. W352E was not expressed as a soluble protein and could not be purified. One explanation for this effect is that a negatively charged residue could not be accommodated in the cavity occupied by W352, suggesting that the cation−π interaction likely served a unique structural function in mediating an interaction between hydrophobic and polar surfaces, which could not be served by other types of weak interactions in protein structures.

The effect of R318A mutation was similar to a previous report (*35*), which also found that the mutation of A316R could partially rescue the mutant of R318A. In PTKs of the Src family, the position equivalent to 316 contains an Arg while the position equivalent to 318 contains an Ala. Examination of the crystal structures of PTKs of the Src family (*14*−*16*) indicated that Arg at 316 (following Csk numbering) also forms the cation−π interaction with W352. We examined if this rescue was due to the restored cation−π interaction, using a double mutant of A316R−R318A. The double mutant A316R−R318A had a k_{cat} of 33.5 min^{-1}, approximately 40% of that of wt, and more than 65-fold higher than that of R318A. The K_m for kdSrc of the double mutant was almost 10 times that of the wt. This result indicated that Arg at 316 could only partially fulfill the function of Arg at 318, but could not rescue the defect in protein substrate binding. The denaturation profile of A316R−R318A was virtually identical to that of R318A (data not shown), indicating that Arg at 316 did not enhance the fluorescence of W352. These results suggested either that Arg at 316 did not form the cation−π interaction with W352 or that the cation−π interaction was not fluorescence-enhancing.

DISCUSSION

The identification and understanding of the network of molecular interactions that are essential for the structure, regulation, and catalysis of PTKs are critical for understanding the mechanisms of signal transduction and developing specific PTK inhibitors. Although crystal structures of several PTKs are now available, detailed structure−function relationships are still not clearly understood. Part of the difficulty rests in the fact that the regulatory and catalytic processes involve dynamic conformational changes to the enzyme and such conformational changes are elusive to investigate. Considering the high sensitivity of intrinsic fluorescence to the environment of Trp residues and conformational changes in proteins, we are interested in probing conformational changes with this powerful technique. In this report, we conducted an initial investigation of the spectral properties of a model PTK, Csk, and further elucidated the structural basis for the observed spectral properties. These studies confirmed that W352 located in the P+1 loop formed a cation−π interaction with R318 in the catalytic loop, and revealed that the cation−π interaction enhanced the fluorescence emission of W352 and caused a significant red shift to the λ_{max} compared to other Trp residues located in a hydrophobic environment. We further demonstrated that the cation−π interaction played a critical role in coupling P+1 loop, responsible for substrate binding, to the catalytic loop, which contains many catalytically essential residues. These studies established correlations of a specific structural feature with the intrinsic fluorescence properties, and the catalytic functions of Csk.

Since W352 and R318 and their cation−π interaction are conserved structural features among all PTKs, urea denaturation and intrinsic fluorescence characterization may be useful techniques in characterizing regulation-related conformational changes in all PTKs. Using the recombinant catalytic domain of IRK, Kohanski and co-workers demonstrated (*25*) that autophosphorylation of IRK alters the intrinsic fluorescence of IRK, and further identified W1175 as the reporter for the conformational changes induced by autophosphorylation. W1175 of IRK is homologous to W352 of Csk. Their study suggests that this cation−π interaction is sensitive to conformational changes in the active site of a PTK due to autophosphorylation.

In addition to forming the cation−π interaction, R318 appears to have other functions, since mutations of R318 had much greater effects (by about 20-fold) on k_{cat} than mutations of W352. To understand this possible additional function for R318, we examined the potential interactions of its corresponding residue, R1136, in the crystal structure of IRK in complex with AMPPNP and peptide substrates (Figure 7B). One of the two ηN atoms of R1136 is about 3.3 Å away from the indole ring, and is apparently forming the cation−π interaction. The other ηN is 2.9 Å from one oxygen of the catalytic base, D1132, while ϵN is 3.1 Å from the phenolic oxygen to be phosphorylated, and 3.9 Å from one γ-phosphoryl oxygen. These additional interactions are likely responsible for additional functions for R318 other than the cation−π interaction. It is interesting to note that even though the catalytic loop in PKA, a Ser/Thr kinase, shares only 50% sequence identity in the catalytic loop with IRK and Csk (Figure 7A), similar interactions in the active site are conserved (Figure 7C). In PKA, E170 occupies the position corresponding to R1136. This negatively charged residue forms a salt-bridge with the Arg at the P-2 position of the peptide substrate (Ser as the 0 position). This interaction couples the catalytic loop with the peptide substrate directly, likely functionally comparable to the cation−π interaction that couples the catalytic loop with the substrate binding P+1 loop. Additional interactions of the R1136 with the catalytic base, the phosphate accepting −OH, and the γ-phosphate of ATP appear to be fulfilled by another positively charged residue, K168, in the catalytic loop in PKA. Such a conservation of interactions between PTKs and PKA even when the primary sequence in the catalytic loop varies dramatically suggests catalytic importance. The recently published (*36*) crystal structure of PKA in complex with a transition-state analogue, AlF_3, reveals that K168 forms a hydrogen bond with one of the fluorides (Figure 7D), further demonstrating the importance of the positive charge of K168 in phosphoryl transfer. Such a comparison between PKA and PTKs favors the notion that R318 (R1136 of IRK) has at least two functions: forming the cation−π interaction with W352 and additional interactions that are also important for catalysis. The details of this additional catalytic function wait to be fully determined. Potentially, the fluorescence yield of W352 due to the cation−π interaction could be used as a reporter to probe the function of R318.

Mutations that disrupted the cation−π interaction had a significant effect on Csk binding of its protein substrate. These data support the notion that the P+1 loop is part of the surface for peptide substrate binding. Csk recognition of PTKs of the Src family is extremely specific—so far, Csk appears to phosphorylate only Src family PTKs in vivo. The mechanisms that ensure this specificity have been controversial and actively investigated (*29*, *37*−*39*). In addition to interactions between the local amino acid sequence surrounding Y527 in Src and the active site of Csk, other interactions between the two molecules also play important roles (*29*). Our results in this current report demonstrated

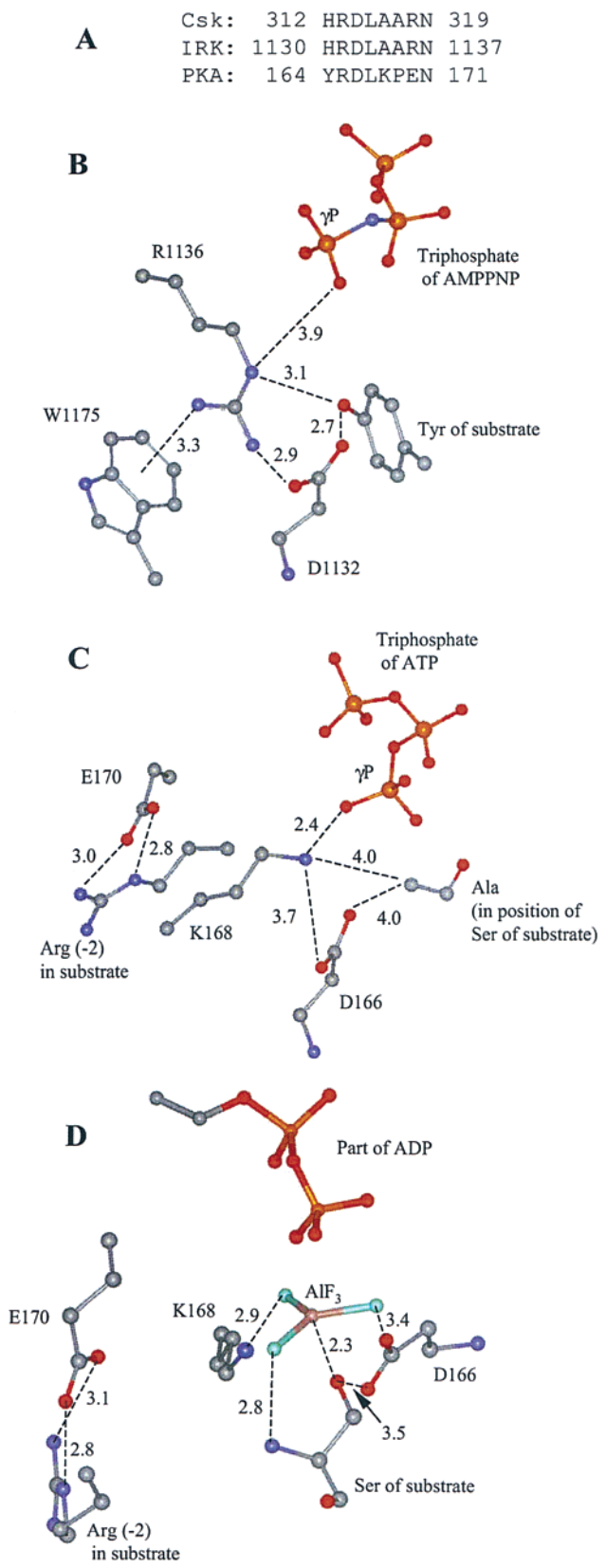

FIGURE 7: Interactions of active site residues in IRK and PKA. (A) Sequence comparison of the catalytic loop in Csk, IRK, and PKA. (B) Interactions in the active site of IRK implying additional functions for R1136. (C) Interactions in the active site of PKA. (D) Interactions in the active site of PKA in complex with a transition-state analogue, ADP, and AlF_3. Only relevant side chains are shown, and distances between relevant atoms are shown in angstroms.

the P+1 loop likely plays an important role in this PTK−substrate recognition.

The cation−π interaction is another weak interaction that stabilizes tertiary structures of proteins, in addition to hydrophobic interactions, salt-bridges, hydrogen bonds, and van der Waals interactions. This interaction has been noted in the crystal structure of a large number of proteins (*34*), and bimolecular interactions (*40, 41*). Results in this current report demonstrated a critical role for this interaction in the active site of a PTK. The effect of the cation on the spectral properties of the π electrons in this interaction is worth noting. Since it is expected that all cation−π interactions involving a Trp will provide a partially polar environment for the Trp residue, enhancement to its fluorescence intensity and red shift of the λ_{max} may be a hallmark of Trp residues involved in cation−π interactions. If proven true, intrinsic fluorescence may be an especially useful method for studying the Trp residues in cation−π interactions. Our results also provided indications of the uniqueness of this interaction. We attempted to determine if a salt bridge can replace the cation−π interaction, by mutating W352 to Glu, but this mutant was unstable, suggesting that a negatively charged residue replacing the hydrophobic Trp would destabilize the protein structure. In contrast, mutation of W352 to Phe, Leu, or Ala merely abolished the cation−π interaction without destabilizing the overall Csk structure. These results indicated that the unique properties of Trp as a hydrophobic side chain that is able to interact with positively charged Arg or Lys residues likely serve a unique role in structural biology.

ACKNOWLEDGMENT

We thank G. Tremblay for interesting and insightful comments and suggestions during the course of this work, and K. Parang, M. Ayrapetov, and J. F. Sperry for critically reading the manuscript. We thank P. A. Cole for providing pREP4groESL plasmid, and R. Jove for providing pMcSrc Met295 plasmid. DNA sequencing was performed at the M. D. Anderson Cancer Center Core Sequencing Facility, supported by an NIH grant (CA16672).

REFERENCES

1. Hunter, T. (1995) *Cell 80*, 225−236.
2. Levitzke, A. (1999) *Pharmacol. Ther. 82*, 231−239.
3. Okada, M., Nada, S., Yamanashi, Y., Yamamoto, T., and Nakagawa, H. (1991) *J. Biol. Chem. 266*, 24249−24252.
4. Mustelin T. (2000) *Src Family Tyrosine Kinases in Leukocytes*, R. G. Landes Co., Austin, TX.
5. Cole, P. A., Sondhi, D., and Kim, K. (1999) *Pharmacol. Ther. 82*, 219−229.
6. Shaffer, J., Sun, G., and Adams, J. A. (2001) *Biochemistry 40*, 11149−11155.
7. Brauninger, A., Holtrich, U., Strebhardt, K., and Rubsamen-Waigmann, H. (1992) *Gene 110*, 205−211.
8. Lamers, M. B., Antson, A. A., Hubbard, R. E., Scott, R. K., and Williams, D. H. (1999) *J. Mol. Biol. 285*, 713−725.
9. Smith, J. A., Francis, S. H., and Corbin, J. D. (1993) *Mol. Cell. Biochem. 127−128*, 51−70.
10. Hubbard, S. R., Mohammadi, M., and Schlessinger, J. (1998) *J. Biol. Chem. 273*, 11987−11990.
11. Klages, S., Adam, D., Class, K., Fargnoli, J., Bolen, J. B., and Penhallow, R. C. (1994) *Proc. Natl. Acad. Sci. U.S.A. 91*, 2597−25601.
12. Hubbard, S. R. (1997) *EMBO J. 16*, 5572−5581.
13. Hubbard, S. R., Wei, L., Ellis, L., and Hendrickson, W. A. (1994) *Nature 372*, 746−754.

14. Yamaguchi, H., and Hendrickson, W. A. (1996) *Nature 384*, 484−489.
15. Xu, W., Harrison, S. C., and Eck, M. J. (1997) *Nature 385*, 595−602.
16. Sicheri, F., Moarefi, I., and Kuriyan, J. (1997) *Nature 385*, 602−609.
17. Plotnikov, A. N., Schlessinger, J., Hubbard, S. R., and Mohammadi, M. (1999) *Cell 98*, 641−650.
18. Schindler, T., Bornmann, W., Pellicena, P., Miller, W. T., Clarkson, B., and Kuriyan, J. (2000) *Science 289*, 1938−1942.
19. Thomas, S. M., and Brugge, J. S. (1997) *Annu. Rev. Cell. Dev. Biol. 13*, 513−609.
20. Brown, M. T., and Cooper, J. A. (1996) *Biochim. Biophys. Acta 1287*, 121−149.
21. Gorinstein, S., Goshev, I., Moncheva, S., Zemser, M., Weisz, M., Caspi, A., Libman, I., Lerner, H. T., Trakhtenberg, S., and Martin-Belloso, O. (2000) *J. Protein Chem. 19*, 637−642.
22. Kleppe, R., Uhlemann, K., Knappskog, P. M., and Haavik, J. (1999) *J. Biol. Chem. 274*, 33251−33258.
23. Ulrich, A., Schmitz, A. A., Braun, T., Yuan, T., Vogel, H. J., and Vergeres, G. (2000) *Proc. Natl. Acad. Sci. U.S.A. 97*, 5191−5196.
24. Leon, D. A., Canaves, J. M., and Taylor, S. S. (2000) *Biochemistry 39*, 5662−5671.
25. Bishop, S. M., Ross, J. B., and Kohanski, R. A. (1999) *Biochemistry 38*, 3079−3089.
26. Smith, D. B., and Johnson, K. S. (1988) *Gene 67*, 31−40.
27. Sun, G., and Budde, R. J. (1995) *Anal. Biochem. 231*, 458−460.
28. Guan, K. L., and Dixon, J. E. (1991) *Anal. Biochem. 192*, 262−267.
29. Wang, D., Huang, X. Y., and Cole, P. A. (2001) *Biochemistry 40*, 2004−2010.
30. Jove, R., Kornbluth, S., and Hanafusa, H. (1987) *Cell 50*, 937−943.
31. Sun, G., and Budde, R. J. (1997) *Biochemistry 36*, 2139−2146.
32. Shibatani, T., Kramer, G., Hardesty, B., and Horowitz, P. M. (1999) *J. Biol. Chem. 274*, 33795−33799.
33. Ogawa, A., Takayama, Y., Sakai, H., Chong, K. T., Takeuchi, S., Nakagawa, A., Nada, S., Okada, M., and Tsukihara, T. (2002) *J. Biol. Chem. 277*, 14351−14354.
34. Gallivan, J. P., and Dougherty, D. A. (1999) *Proc. Natl. Acad. Sci. U.S.A. 96*, 9459−9464.
35. Williams, D. M., Wang, D., and Cole, P. A. (2000) *J. Biol. Chem. 275*, 38127−38130.
36. Madhusudan, A. P., Xuong, N. H., and Taylor, S. S. (2002) *Nat. Struct. Biol. 9*, 273−277.
37. Sun, G., and Budde, R. J. (1999) *Arch. Biochem. Biophys. 367*, 167−172.
38. Sondhi, D., Xu, W., Songyang, Z., Eck, M. J., and Cole, P. A. (1998) *Biochemistry 37*, 165−172.
39. Amrein, K. E., Molnos, J., zur Hausen, J. D., Flint, N., Takacs, B., and Burn, P. (1998) *Farmaco 53*, 266−272.
40. Tokita, K., Katsuno, T., Hocart, S. J., Coy, D. H., Llinares, M., Martinez, J., and Jensen, R. T. (2001) *J. Biol. Chem. 276*, 36652−36663.
41. Pletneva, E. V., Laederach, A. T., Fulton, D. B., and Kostic, N. M. (2001) *J. Am. Chem. Soc. 123*, 6232−6245.

BI026439G